Finite-Element Analysis of Coupled Thermoviscoelastic Structures Undergoing Sustained Periodic Vibrations

Thomas L. Cost*
University of Alabama, Tuscaloosa, Ala.
and
James M. Heard†
U.S. Air Force Armament Laboratory, Eglin Air Force Base, Fla.

A general method is presented for analyzing the effects of internal heating in geometrically complex viscoelastic structures due to exposure to sustained periodic vibratory loads. The analysis employs the finite-element method for both transient displacement and temperature determinations and utilizes "complex" viscoelastic material property functions. The method is demonstrated by application to a problem involving longitudinal oscillations of a linear viscoelastic rod. General agreement is obtained with the results of Huang and Lee which appear in the literature. The method is applicable to geometrically complex, linear viscoelastic structures of the thermorheologically simple type undergoing small deformations. Existing computer codes that model liner elastic materials can be used, with minor modifications, to obtain linear viscoelastic results.

I. Introduction

THE heat generated in viscoelastic materials subjected to long-duration vibratory loads is of concern in many applications. Such common items as gears, bellows, mechanical couplings, bearing pads, and vibration absorbers are polymeric materials exposed to sustained cyclic loads. Epoxy aircraft and automobile parts often are subjected to sustained vibrations. Missiles containing viscoelastic solid rocket grains often are mounted on fixed-wing aircraft and helicopters, where they experience vibrations. Such an application is illustrated in Fig. 1, where the complex solid rocket grain is shown with a grid superimposed for a finite-element analysis. The heat generated in such structures as a result of the sustained vibration can result in a degradation of the strength and stiffness of a viscoelastic structure[1] or in thermal decomposition of the vibrating material. This phenomenon has been of interest to several investigators, notably Schapery,[2] Petrof and Gratch,[3] Huang and Lee,[4] Tauchert,[5] and Cost.[6,7] Oden and Armstrong[8] have presented a general method for solving dynamic, nonlinear, coupled thermoviscoelastic problems which appears best suited for short-time transient coupled behavior. Solutions expressed in terms of time-dependent material properties appear to be not well suited for sustained periodic vibrations; frequency-dependent viscoelastic properties appear more appropriate.

To the present time, solution procedures for coupled problems involving sustained periodic motions have been restricted to one-dimensional geometries or have ignored inertia effects.[1-7] The objective of this paper is to describe a method for solving dynamic coupled thermoviscoselastic problems undergoing sustained periodic motions which is applicable to geometrically complex structures. The method can utilize existing elastic computer codes, with modifications, to obtain the viscoelastic results.

Received Sept. 6, 1977; revision received May 17, 1978.

Index categories: Structural Design; Thermal Stresses; Solid and Hybrid Rocket Engines.

*Professor, Dept. of Aerospace Engineering, Mechanical Engineering, and Engineering Mechanics.

†Research Engineer, Vulnerability Analysis Section.

II. Cyclic Loading Analysis

Consider a viscoelastic body subject to transient loading conditions. The deviatoric components of the stress and strain tensors are defined, respectively, as

$$s_{ij} = \sigma_{ij} - 1/3\,\delta_{ij}\alpha_{kk} \tag{1}$$

$$e_{ij} = \epsilon_{ij} - 1/3\,\delta_{ij}\epsilon_{kk} \tag{2}$$

where σ_{ij} is a component of the Cauchy stress tensor and ϵ_{ij} is a component of the small strain tensor. If the transient loads are steady-state harmonic functions of time, the stress and strain can be expressed as the real or imaginary parts of

$$\sigma_{lm} = \bar{\sigma}_{lm}(\underset{\sim}{x})\,e^{i\omega t} \tag{3}$$

$$\epsilon_{lm} = \bar{\epsilon}_{lm}(\underset{\sim}{x})\,e^{i\omega t} \tag{4}$$

where $\bar{\sigma}_{lm}(\underset{\sim}{x})$ and $\bar{\epsilon}_{lm}(\underset{\sim}{x})$ are, strictly speaking, slowly varying functions of time due to the slowly varying temperature. However, since this variation is extremely slow in comparison with the period of the vibratory motion, it need not be considered in either the deviatoric or dilatational stress-strain relations, which may be expressed as

$$\bar{s}_{lm}(\underset{\sim}{x}) = 2\mu^*(i\omega)\,\bar{e}_{lm}(\underset{\sim}{x}) \tag{5}$$

$$\bar{\sigma}(\underset{\sim}{x}) = 3k^*(i\omega)\,\bar{\epsilon}(\underset{\sim}{x}) \tag{6}$$

where

ω = frequency of oscillation
$\mu^*(i\omega)$ = complex shear modulus
$k^*(i\omega)$ = complex bulk modulus
$\bar{\sigma}$ = hydrostatic stress component
$\bar{\epsilon}$ = dilatation component

It can be seen from Eqs. (5) and (6) that the stress-strain relations for a linear viscoelastic material subject to steady-state harmonic loads or displacements have the same form as those for a linear elastic material, except that now all of the quantities, including the material properties, are complex.

By standard finite-element techniques,[9] the discrete equations of motion for for a linear elastic solid can be expressed as

$$\underset{\approx}{M}\,\ddot{\underset{\sim}{u}} + \underset{\approx}{K}\,\underset{\sim}{u} = \underset{\sim}{F} \tag{7}$$

where

$\underset{\sim}{u}$ = vector of nodal point displacements
$\ddot{\underset{\sim}{u}}$ = acceleration vector
$\underset{\sim}{F}$ = applied load vector
$\underset{\approx}{M}$ = structural mass matrix
$\underset{\approx}{K}$ = structural stiffness matrix

Using the arguments just described for steady-state periodic forcing functions, we see that the corresponding finite-element equations of a linear viscoelastic structure can be expressed as

$$-\omega^2 \underset{\approx}{M} \bar{\underset{\sim}{u}} + \underset{\approx}{K}^* \bar{\underset{\sim}{u}} = \bar{\underset{\sim}{F}} \tag{8}$$

where $\bar{\underset{\sim}{u}}$ and $\bar{\underset{\sim}{F}}$ are complex quantities defined by the relations

$$\underset{\sim}{u} = \bar{\underset{\sim}{u}} e^{i\omega t} \tag{9}$$

$$\underset{\sim}{F} = \bar{\underset{\sim}{F}} e^{i\omega t} \tag{10}$$

and $\underset{\approx}{K}^*$ is the complex stiffness matrix obtained from $\underset{\approx}{K}$ by inserting the complex viscoelastic material properties for the corresponding elastic properties. By separating all complex quantities in Eq. (8) into real and imaginary parts and equating the real and imaginary parts, there results a matrix equation of the form

$$\begin{bmatrix} (-\omega^2 \underset{\approx}{M} + \underset{\approx}{K}') & (\underset{\approx}{K}'') \\ \underset{\approx}{K}'' & (\omega^2 \underset{\approx}{M} - \underset{\approx}{K}') \end{bmatrix} \begin{Bmatrix} \underset{\sim}{u}' \\ \underset{\sim}{u}'' \end{Bmatrix} = \begin{Bmatrix} \underset{\sim}{F}' \\ \underset{\sim}{F}'' \end{Bmatrix} \tag{11}$$

where

$$\bar{\underset{\sim}{u}} = \underset{\sim}{u}' + i\underset{\sim}{u}'' \tag{12}$$

$$\bar{\underset{\sim}{F}} = \underset{\sim}{F}' + i\underset{\sim}{F}'' \tag{13}$$

$$\underset{\approx}{K} = \underset{\approx}{K}' + i\underset{\approx}{K}'' \tag{14}$$

Equation (11) represents the finite-element matrix equation for a visco-elastic body undergoing cyclic loading. The "storage" stiffness component $\underset{\approx}{K}'$ and "loss" stiffness component $\underset{\approx}{K}''$ are both dependent on the frequency of oscillation, since the material properties $\mu^*(i\omega)$ and $k^*(i\omega)$ are frequency-dependent. If the viscoelastic material is assumed to be thermorheologically simple, μ^* and k^* also depend on temperature through relations of the form

$$\mu^*(i\bar{\omega}) = \mu^*[i\omega\alpha(T)] \tag{15}$$

$$k^*(i\bar{\omega}) = k^*[i\omega\alpha(T)] \tag{16}$$

where $\bar{\omega}$ is the reduced frequency, and $\alpha(T)$ is a temperature-dependent shift factor.[4] Since the temperature, in general, varies from point to point in the body, each finite element has a particular value of temperature T, shift factor $\alpha(T)$, and reduced frequency $\bar{\omega}$ associated with it. Consequently, each element of the stiffness matrices $\underset{\approx}{K}'$ and $\underset{\approx}{K}''$ must be modified to accomodate varying temperature distributions. Provided that the temperature distribution is known at a particular time, Eq. (11) can be used to calculate the displacements at various points in the body which, in turn, can be used to calculate the resultant strains and stresses throughout the body. It remains to develop a process for determining the transient temperature distributions resulting from the dissipation effects.

III. Heat-Conduction Analysis

It has been shown that the equation governing transient heat conduction with thermomechanical dissipation effects present can be expressed as[7]

$$kT_{,ii} = \rho c \dot{T} - \bar{Q} \tag{17}$$

where the subscripts following a comma denote differentiation with respect to the spatial coordinate x_i and the dots over a quantity denote differentiation with respect to time, and where

T = temperature
c = specific heat at constant volume
ρ = density
k = thermal conductivity
$\bar{Q}$ = cycle-averaged dissipation function

The cycle-averaged dissipation function can be expressed as

$$\bar{Q} = \frac{\omega}{2\pi} \int_t^{t+(2\pi/\omega)} \sigma_{ij} \dot{\epsilon}_{ij} \mathrm{d}t' \tag{18}$$

where, as before, σ_{ij} and ϵ_{ij} are stress and strain tensor components, respectively, and ω is the circular frequency of oscillation.

Employing conventional finite-element methodology,[10] the partial differential equation (17) can be expressed in matrix form as

$$\underset{\approx}{H}\underset{\sim}{T} + \underset{\approx}{C}\dot{\underset{\sim}{T}} = \underset{\sim}{q}^* + \underset{\sim}{Q}^* \tag{19}$$

where

$\underset{\sim}{T}$ = vector of nodal point temperatures
$\underset{\approx}{H}$ = conductivity matrix
$\underset{\approx}{C}$ = specific heat matrix
$\underset{\sim}{q}^*$ = boundary heat flux vector
$\underset{\sim}{Q}^*$ = internal heat-generation vector

Various time-marching schemes can be used to reduce Eq. (19) to a set of algebraic equations. By expanding the temperature in a Taylor series in time about a point $t = t_i$ and assuming

$$\ddot{\underset{\sim}{T}}(t_i) = [\dot{\underset{\sim}{T}}(t_{i+1}) - \dot{\underset{\sim}{T}}(t_i)]/\Delta t \tag{20}$$

the following relation can be obtained:

$$(\dot{\underset{\sim}{T}}_{i+1} + \dot{\underset{\sim}{T}}_i) = (2/\Delta t)(\underset{\sim}{T}_{i+1} - \underset{\sim}{T}_i) \tag{21}$$

In Eq. (21), Δt is used to denote $(t_{i+1} - t_i)$, and $\underset{\sim}{T}(t_i)$ has been shortened to $\underset{\sim}{T}_i$. At times t_i and t_{i+1}, Eq. (19) becomes

$$\underset{\approx}{H}\underset{\sim}{T}_i + \underset{\approx}{C}\dot{\underset{\sim}{T}}_i = \underset{\sim}{q}^* + \underset{\sim}{Q}_i^* = \underset{\sim}{f}_i \tag{22}$$

$$\underset{\approx}{H}\underset{\sim}{T}_{i+1} + \underset{\approx}{C}\dot{\underset{\sim}{T}}_{i+1} = \underset{\sim}{q}_{i+1}^* + \underset{\sim}{Q}_{i+1}^* = \underset{\sim}{f}_{i+1} \tag{23}$$

Adding Eqs. (22) and (23) and employing Eq. (21) yields

$$[\underset{\approx}{H} + (2/\Delta t)\underset{\approx}{C}]Z_i = \underset{\sim}{P}_i \tag{24}$$

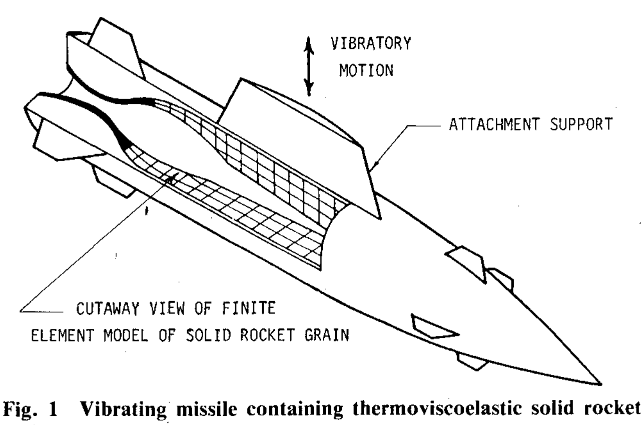

Fig. 1 Vibrating missile containing thermoviscoelastic solid rocket grain.

where

$$\underset{\sim}{Z}_i = \tfrac{1}{2}(\underset{\sim}{T}_{i+1} + \underset{\sim}{T}_i) \tag{25}$$

$$\underset{\sim}{P}_i = \tfrac{1}{2}(\underset{\sim}{f}_{i+1} + \underset{\sim}{f}_i) + (2/\Delta t)\underset{\approx}{C}\underset{\sim}{T}_i \tag{26}$$

At time t_i, the temperature $\underset{\sim}{T}_i$ and forcing functions $\underset{\sim}{f}_{i+1}$ and $\underset{\sim}{f}_i$ are known, and Eq. (24) can be used to solve for $\underset{\sim}{Z}_i$. The temperature at the next time step $\underset{\sim}{T}_{i+1}$ then is obtained from Eq. (25). Applying this method repeatedly for small time steps allows the temperature solution to be advanced in time.

IV. Summary of Method

The basic procedure to be followed to obtain a solution to the coupled thermomechanical problem is as follows:

1) Using the specified initial temperatures, calculate the appropriate material properties $\mu^*[i\omega\alpha(T)]$ and $k^*[i\omega\alpha(T)]$.

2) Use Eq. (11) to solve for the displacements within the body at time zero.

3) Use difference relations to calculate the strains and the stress-strain relations, Eqs. (5) and (6), to calculate the stresses within each element.

4) Evaluate the dissipation function for the next time step using Eq. (18) and the stresses and strains at the current time.

5) Solve for the nodal point temperatures at the next time step using Eqs. (24) and (25).

6) Modify the material properties within each element based upon the local temperature, and use Eq. (11) to solve for the displacements at the next time step.

7) Repeat steps 3 and 6 for as many time steps as are of interest.

V. Results

To demonstrate the general technique described in the preceding sections, the method has been applied to a specific problem. Consider a viscoelastic rod of finite length L insulated on its lateral surface as shown in Fig. 2. The origin $x=0$ is located at the left end of the rod. The right end is subjected to a prescribed stress of the form $\sigma = \sigma_0 \cos\omega t$, where σ_0 is constant, ω reflects the frequency of stressing, and t is time. The right end of the rod is maintained at a constant temperature T_0, and the temperature at the left hand end is assumed to satisfy a radiation-type boundary condition of the form

$$\frac{\partial T}{\partial x} = C_1(T - T_0) \tag{27}$$

where C_1 is the ratio of surface conductance to thermal conductance of the viscoelastic material. The initial temperature is uniform and has a magnitude T_0.

The finite-element model used to describe the rod is one-dimensional. Element stiffness and conductivity matrices are based upon linear functions. In global coordinates, the detailed governing equations equivalent to the general Eqs. (11) are a banded set of equations of the form

$$\begin{bmatrix} \underset{\approx}{B}_1 & \underset{\approx}{C}_1 & & & & \\ \underset{\approx}{A}_2 & \underset{\approx}{B}_2 & \underset{\approx}{C}_2 & & & \\ & \underset{\approx}{A}_3 & \underset{\approx}{B}_3 & \underset{\approx}{C}_3 & & \\ & & & \ddots & & \\ & & & \underset{\approx}{A}_{n-1} & \underset{\approx}{B}_{n-1} & \underset{\approx}{C}_{n-1} \\ & & & & \underset{\approx}{A}_n & \underset{\approx}{B}_n \end{bmatrix} \begin{bmatrix} \underset{\sim}{U}_1 \\ \underset{\sim}{U}_2 \\ \underset{\sim}{U}_3 \\ \vdots \\ \underset{\sim}{U}_{n-1} \\ \underset{\sim}{U}_n \end{bmatrix} = \begin{bmatrix} \underset{\sim}{F}_1 \\ \underset{\sim}{F}_2 \\ \underset{\sim}{F}_3 \\ \vdots \\ \underset{\sim}{F}_{n-1} \\ \underset{\sim}{F}_n \end{bmatrix} \tag{28}$$

where

$$\underset{\approx}{A}_j = \begin{bmatrix} -\omega^2\Gamma_1 - \Gamma_2 & -\Gamma_3 \\ -\Gamma_3 & \omega^2\Gamma_1 + \Gamma_2 \end{bmatrix}, \quad j \neq 1,\ j \neq n \tag{29}$$

$$\underset{\approx}{B}_j = \begin{bmatrix} -4\omega^2\Gamma_1 + 2\Gamma_2 & 2\Gamma_3 \\ 2\Gamma_3 & 4\omega^2\Gamma_1 - 2\Gamma_2 \end{bmatrix}, \quad j \neq 1,\ j \neq n \tag{30}$$

$$\underset{\approx}{C}_j = \underset{\approx}{A}_{j+1} \tag{31}$$

$$\underset{\approx}{B}_1 = \underset{\approx}{B}_n = (1/2)\underset{\approx}{B}_j \tag{32}$$

Also, in Eqs. (29) and (30),

$$\Gamma_1 = 1/6\rho(\Delta x)A \tag{33}$$

$$\Gamma_2 = AE'/\Delta x \tag{34}$$

$$\Gamma_3 = AE''/\Delta x \tag{35}$$

where

ρ = material density
A = rod cross-sectional area
Δx = length of finite element
E' = storage modulus in tension
E'' = loss modulus in tension

The quantities E' and E'' are temperature-dependent as well as frequency-dependent and thus vary from one element to another within the rod. They must be changed as the temperature of the element changes. The displacements and forces in Eq. (28) are defined as

$$\underset{\sim}{U}_j = \begin{Bmatrix} u_j' \\ u_j'' \end{Bmatrix} \tag{36}$$

$$\underset{\sim}{F}_j = \begin{Bmatrix} f_j' \\ -f_j'' \end{Bmatrix} \tag{37}$$

where u_j' and u_j'' are real and imaginary components of the nodal point displacements, and f_j' and f_j'' are the corresponding nodal point forces. Once the nodal point displacements have been obtained from Eq. (28), the strains can be evaluated using difference equations and the stresses by use of the stress-strain relations.

For the one-dimensional case under consideration here, the dissipation function $\bar{Q}$ in Eq. (18) reduces to

$$\bar{Q} = \tfrac{1}{2}\omega\,|\epsilon_{max}|^2 E''(i\bar{\omega}) \tag{38}$$

where $|\epsilon_{max}|$ is the magnitude of the maximum longitudinal cyclic strain with each element.

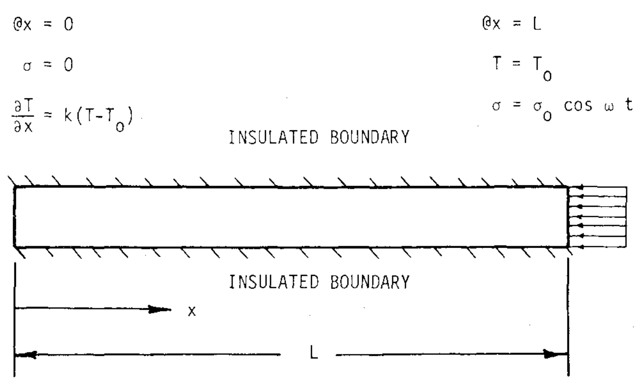

Fig. 2 Boundary conditions for vibrating rod.

Results were obtained for this problem utilizing material properties and numerical constants that coincide with a solution obtained by Huang and Lee.[4] The material properties were specified by Huang and Lee to be of the form

$$D' = \lambda_1 \omega^{\beta} (T - T_1) \alpha \tag{39}$$

$$D'' = \lambda_2 \omega^{\beta} (T - T_1) \alpha \tag{40}$$

where λ_1, λ_2, β and α are constants, T_1 is a reference temperature, and where D' and D'' are the real and imaginary parts of the complex tensile compliance D^*. Using standard interrelationships between viscoelastic properties,[2] D' and D'' can be used to calculate E' and E''. Note that Eqs. (39) and (40) have the temperature dependence included in the material property specifications.

Numerical solutions were obtained for the specific parameters listed below:

$\lambda_1 = 6.6860\,(TPa)^{-1}$	$\lambda_2 = 2.3495\,(TPa)^{-1}$
$\beta = -0.214$	$\alpha = 3.21$
$C_1 = 1.3122\ \mathrm{m}^{-1}$	$T_0 = 18.33°\mathrm{C}$
$T_1 = -51.67°\mathrm{C}$	$L = 7.62\ \mathrm{cm}$
$\rho = 12{,}156\ \mathrm{kg/m^3}$	$\omega = 10^4\ \mathrm{rad/s}$
$k = 3.6408 \times 10^{-4}\ \mathrm{cal/cm\text{-}s\text{-}°C}$	$c = 0.389\ \mathrm{cal/g\text{-}°C}$

These mechanical and thermal properties are taken from Ref. 4 and correspond to the behavior of a solid-propellant material. The magnitude of the stress acting on the right end was assumed to be $\sigma = 9.86$ kPa. To assess the adequacy of the finite-element method for determining the stress in the rod, independent of the temperature calculation, the quantities $\sigma_1(x)$ and $\sigma_2(x)$ were calculated for time zero conditions when the temperature is uniform. The actual stress at any point in the rod at any time can be expressed as

$$\sigma_x(x,t) = \sigma_1(x)\cos\omega t - \sigma_2(x)\sin\omega t \tag{41}$$

The values of $\sigma_1(x)$ and $\sigma_2(x)$ illustrated in Fig. 3 were calculated using 60 equal-length elements to describe the 7.62-cm rod under consideration. The finite-element stress results agree closely with the analytical results obtained by Huang and Lee for this condition.

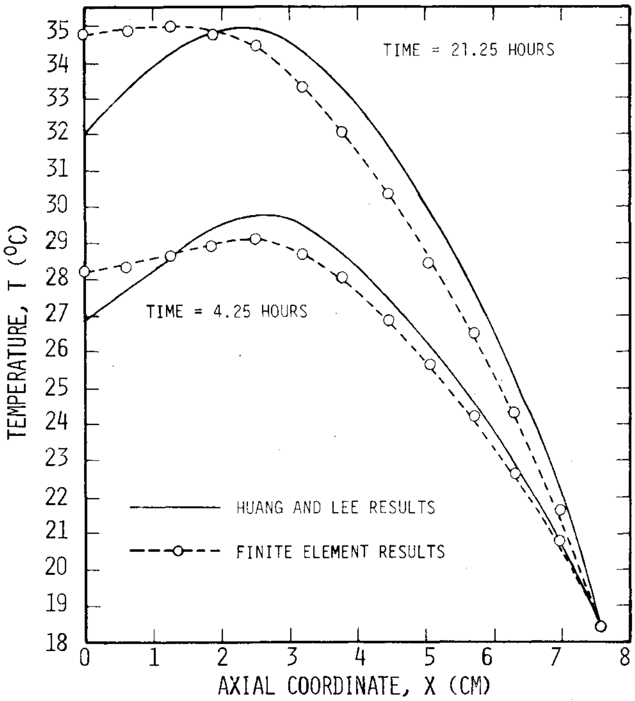

Fig. 4 Temperature distribution in rod at times of 4.25 and 21.25 h.

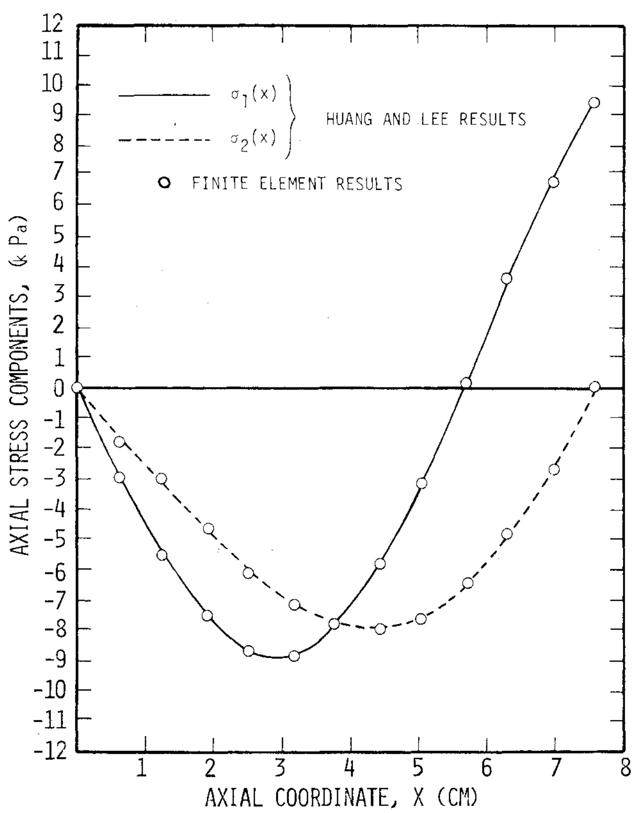

Fig. 3 Stress distribution in rod at time zero.

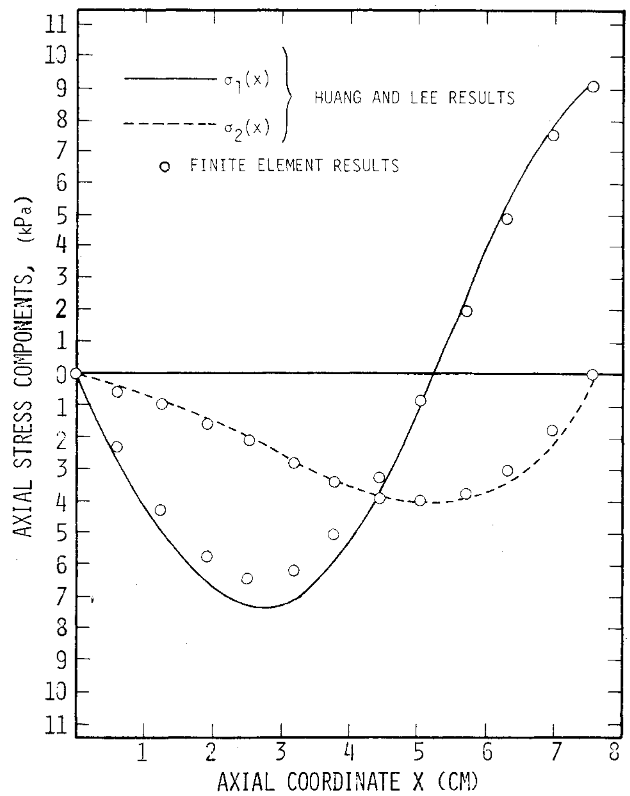

Fig. 5 Stress distribution in rod at time of 4.25 h.

Difficulty was encountered in trying to reproduce the Huang and Lee results for the temperature distribution, as illustrated in Fig. 3. These results are for a time of 4.25 h and were obtained using a time increment of 0.05 h. The disagreement seems to be primarily a result of the approximation of the radiation boundary condition at the left end of the rod. To check the finite-element results, two methods were utilized to model this boundary condition. First, a three-point, forward-difference equation was used to develop an expression for $\partial T/\partial x$ in terms of discrete values. The matrix equations then were modified to reflect this constraint condition. Second, the term $k(\partial T/\partial x)$, which represents the heat flux at the left end of the rod and, consequently, the corresponding forcing function of the right-hand side of the governing matrix equations, was modified to reflect the radiation condition constraint. Both methods resulted in temperature predictions that agreed with each other to four significant figures. Other difference methods were used to model the radiation boundary condition. However, none of the results agreed exactly with those of Huang and Lee, who used finite-difference methods to compute both the temperature and stress distributions at various times. The specific difference relation employed by Huang and Lee to model the radiation boundary condition is not described in their paper. Steady-state conditions occur at a time of 21.25 h. The temperature predictions at this time also are shown in Fig. 4.

Since the material properties of the rod depend upon the local temperature, the stresses are also dependent upon the local temperature. Hence, the finite-element results would be expected to differ from the Huang and Lee results, since the temperature predictions differ. Figure 5 illustrates the magnitude of this difference in stress at a time of 4.25 h. The steady-state distributions are similar.

VI. Discussion

The method presented appears to be well suited for the analysis of geometrically complex bodies with inertia effects included. Existing elastic finite-element codes can be used to generate the stiffness matrices in Eq. (11), with the frequency-dependent viscoelastic material properties substituted for the elastic properties. Lumped mass matrices can be calculated without much difficulty for combining with the stiffness matrices, as in Eq. (11).

The method presented is limited to vibrations that are periodic functions of time. If the vibrations are random, other developments are needed for the dissipation function, and the method for computing the displacements, strains, and stresses in the body must be modified. The method also is limited to small strain applications and linear viscoelastic material behavior. For nonlinear applications, refinements must be made in the dissipation function expression and solution method.

Acknowledgment

Support of this work by the U.S. Air Force Office of Scientific Research under Contract F44620-69-C-0124 is gratefully acknowledged.

References

[1] Tormey, J. F. and Britton, S. C., "Effect of Cyclic Loading on Solid Propellant Grain Structures," *AIAA Journal*, Vol. 1, Aug. 1963, pp. 1763-1770.

[2] Schapery, R. A. and Cantey, D. E., "Thermomechanical Response Studies of Solid Propellants Subject to Cyclic and Random Loading," *AIAA Journal*, Vol. 4, Feb. 1966, pp. 255-264.

[3] Petrof, R. C. and Gratch, S., "Wave Propagation in a Viscoelastic Material with Temperature-Dependent Properties and Thermomechanical Coupling," *Journal of Applied Mechanics*, Vol. 86, Ser. E, 1964, pp. 423-429.

[4] Huang, N. C. and Lee, E. H., "Thermomechanical Coupling Behavior of Viscoelastic Rods Subjected to Cyclic Load," *Journal of Applied Mechanics*, Vol. 89, Ser. E, March 1967, pp. 127-132.

[5] Tauchert, T. R., "Transient Temperature Distributions in Viscoelastic Solids Subject to Cyclic Deformations," *Acta Mechanica*, Vol. 6, 1968, pp. 239-252.

[6] Cost, T. L. and Hill, J. L., "Thermomechanical Dissipation Analysis of Thermoviscoelastic Solids by Finite Elements," *Developments in Theoretical and Applied Mechanics, Sixth Southeastern Conference on Theoretical and Applied Mechanics*, edited by E. G. Henneke II and S. C. Kranc, Vol. 6, 1972, pp. 727-759.

[7] Cost, T. L., "A Free Energy Functional for Thermorheologically Simple Materials," *Acta Mechanica*, Vol. 17, 1973, pp. 153-167.

[8] Oden, J. T. and Armstrong, W. H., "Analysis of Nonlinear, Dynamic Coupled Thermoviscoelasticity Problems by the Finite Element Method," *Computers and Structures*, Vol. 1, 1971, pp. 603-621.

[9] Zienkiewicz, O. C. and Cheung, Y. K., *The Finite Element Method in Structural and Continuum Mechanics*, McGraw-Hill, New York, 1967, pp. 170-171.

[10] Wilson, E. L., Nickell, R. E., "Application of the Finite Element Method to Heat Conduction Analysis," *Nuclear Engineering and Design*, Vol. 4, March 1966, pp. 276-286.